EnvironmentAsia
The international journal published by the Thai Society of Higher Education Institutes on Environment

Available online at www.tshe.org/ea/index.html
EnvironmentAsia 10(2) (2017) 126-134
DOI

Photocatalytic Degradation of 2, 4-dichlorophenol using N-doped SnO_2/TiO_2 Thin Film Coated Glass Fibers

Peerawas Kongsong [a], Lek Sikong [b] and Mahamasuhaimi Masae [c]

[a] *Department of Materials Engineering, Faculty of Engineering and Architecture, Rajamangala University of Technology Isan, Nakhon Ratchasima 30000, Thailand*
[b] *Department of Mining and Materials Engineering, Faculty of Engineering,Prince of Songkla University, Hat Yai, Songkhla 90112, Thailand*
[c] *Department of Industrial Engineering, Faculty of Engineering, Rajamangala University of Technology Srivijaya, Songkla 90000, Thailand*

Abstract

Photocatalytic degradation of 2,4-dichlorophenol (2,4-DCP) contaminant in water was investigated. Composite SnO_2/TiO_2 films N-doped to varying degrees were prepared via sol-gel method, and coated on glass fibers by dipping method.The effects of nitrogen-doping on coating morphology, physical properties, and 2,4-DCP degradation rates were experimentally determined. Nitrogen-doping shifted absorption wavelengths and narrowed the energy band gap, enhancing photocatalytic performance. The maximum efficiency of 2,4-DCP degradation was up to 93.65% for 12 h of $40N/SnO_2/TiO_2$ composite film. The near optimal $40N/SnO_2/TiO_2$ composite thin film exhibited about 4 folds degradation rates relative to pure TiO_2, and should perform well in water purification applications.

Keywords: N-doped SnO_2/TiO_2; sol-gel methods; glass fibers; 2,4-DCP

1. Introduction

One of the most important sources of environmental pollutionare organic pollutants that they are the major threats to the environment, human and animal health, especially water resources. These substances are non-biodegradable and stable and need to be removed from the environment (Hoseini *et al*., 2017). 2,4-Dichlorophenol (2,4-DCP) is a chemical precursor for manufacture of a widely used herbicide 2,4-dichlorophenoxy acetic acid (2,4-DCP). After the herbicide have been applied on agricultural sites, 2,4-DCP is the major transformation product of 2,4-D by solar photolysis and/or microbial activities in the nearby soil or in natural water. 2,4-DCP has also been found in disinfected water after chlorination, in the flue gas of municipal waste incineration, or in pulp and paper wastewater. It has been realized that 2,4-DCP may cause some pathological symptoms and changes to endocrine systems of human (Li *et al*., 2007). The removal of these hazardous organic pollutants has become necessary and important for environmental safety. These organic compounds can be oxidized using chemical, photochemical and microbiological processes (Sinirtas *et al*., 2016).

Conventional processes, such as physical, chemical and biological methods, are used to remove chlorophenols. These techniques, however, are difficult to degrade such refractory biodegradation organic pollutants completely. In recent years, several advanced oxidation processes (AOPs) are put forward for the degradation of chlorophenols. One of the most important photocatalysts is titaniumdioxide (TiO_2), which has been known as the most preferable photocatalyst due to its stability, nontoxicity, and low cost. (Jian *et al*., 2013). TiO_2, as a photocatalyst, has been studied for its high catalytic efficiency, non-toxicity and stable chemical performance. However, it is difficult for TiO_2 powder to disperse and be recycled in aqueous solution, TiO_2 is mostly coated on some carriers before use. When it is irradiated by photon whose energy exceeded 3.2 eV, holes that have powerful oxidation ability and electrons that have reduction ability are both generated on the surface of TiO_2, but recombination of holes and electrons occurs at the same time, reducing the catalytic performance of TiO_2. In order to enhance TiO_2 catalytic ability, it is modified by adulterating metal ions or some metal oxides to restrict or reduce the recombination efficiency. There are some

reports on the catalytic application of TiO_2. However, reports about the association degradation of organic with TiO_2 and others processes are mostly simple. (Zhao *et al*., 2007)

In order to enhance the photocatalytic activity of TiO_2 for its practical use and commerce, it is important to decrease the recombination of photogenerated charge carriers. Coupling TiO_2 with other semiconductors can provide a beneficial solution for this drawback. For example, Tada *et al*. (2004) and Kadam *et al*. (2017) conducted a systematic research on the SnO_2 as a coupled semiconductor and confirmed that the photogenerated electrons in the SnO_2/TiO_2 system can accumulate on the SnO_2 and photogenerated holes can accumulate on the TiO_2 because of the formation of heterojunction at the SnO_2/TiO_2 interface, which can result in lower recombination rate of photogenerated charge carriers and higher quantum efficiency and better photocatalytic activity (Zhou *et al*., 2008).

Nitrogen-doped titanium dioxide is attracting a continuously increasing attention because of its potential the material for environmental photocatalysis. Many authors have reported that N-doped titanium dioxide. While some authors claim that the band gap of the solid is reduced due to a rigid valence band shift upon doping, others attribute the observed absorption of visible light by N-TiO_2 to the excitation of electrons from localized impurity states in the band-gap. Interestingly, it appears that the N-doping induced modifications of the electronic structure may be slightly different for the anatase and rutile polymorphs of TiO_2. The mechanism of N-dopant influence on the photoabsorption and photoactivity was a matter of intensive discussions. Various theoretical and experimental approaches assuming band gap narrowing by overlapping between N 2p and O 2p orbitals, e.g, formation of intra-band surface states, oxygen vacancies, demonstrate the complexity of the case and deserved several reviews, as for example. It is reminded that N doping is extremely sensitive to the preparation technique and its state and configuration is still in the focus of researcher's attention. A number of investigations of substitutional and interstitial N-doped TiO_2 visible light photocat-alytic activity confirms the advantage of interstitial position (Valentin *et al*., 2007; Georgieva *et al*., 2017).

The aim of this work is to assess the degradation of 2,4-DCP contaminant in water by photocatalytic treatments, using N-doped SnO_2/TiO_2 composites and TiO_2 a baseline, coated on glass fibers. An optimum level of nitrogen-doping was determined, for maximizing the degradation rate of 2,4-DCP The films were also characterized for their morphology, anatase crystallinity, and band gap energy and considered fundamental explanatory characteristics affecting photocatalytic activity.

2. Experimenta

2.1 Materials and methods

Three coating layers were deposited on glass fibers of type E-glass by the sol-gel process using the dip-coating method. The specific surface area of the starting glass fiber materials is 0.05 m^2g^{-1} and diameter is about 20 μm. The coating sol for the first layer film was a SiO_2/TiO_2, prepared by dissolving 9 mL titanium tetra-isopropoxide (TTIP, 99.95%, Fluka Sigma-Aldrich) and 0.07 mL tetraethylorthosilicate (TEOS, 98%, Fluka Sigma-Aldrich) with 145 mL ethanol, stirring at room temperature with a speed of 800 rpm for 60 min to achieve the mole ratio of TTIP:C_2H_5OH = 1:82 then adding 2 M HCl into the sol to adjust pH to be about 3.5. The coating sol for the second and third layers were the N-doped SnO_2/TiO_2 composite, prepared by dissolving certain amounts of TTIP, polyvinylprrolidone (PVP), and 0.315 g tin (IV) chloride pentahydrate (98%, Riedel DeHaën) with 145 mL ethanol, stirring at room temperature with a speed of 800 rpm for 60 min then adding 2 M HCl into the sol to adjust pH to be about 3.5. The concentration of SiO_2 in TiO_2 of the first layer was fixed at 5 mol%, while in the second and third layer 3 mol% SnO_2 was used (Kongsong *et al*., 2014). Nitrogen of 0-40 mol% was doped into the SnO_2/TiO_2 composite films following Hao-Li Qin and co-workers (Qin *et al*., 2008).

Before coating, the glass fibers were heated at 500°C for 1 h in order to remove wax, cleaned in an ultrasonic bath by using ethanol and dried at 105°C for 24 h. A dip-coating apparatus was used to coat the fibers. Firstly, SiO_2/TiO_2 sol was coated on glass fibers as a compatibilizer layer and followed with N-doped SnO_2/TiO_2 sol on top for another two layers. The sol could be homogenously coated on the substrate at the dipping speed of 1.0 mm/s. Secondly, gel films of TiO_2 composites were obtained by drying at 60°C for 30 min before calcination at 600°C for 2 h at a heating rate of 10°C/min. After that the TiO_2 composite films coated glass fibers were cleaned with distilled water in an ultrasonic bath for 15 min in order to remove the TiO_2 free particles, dried at 105°C for 24 h and kept in a desiccator until use in experiments (Kongsong *et al*., 2014).

2.2 Materials characterization

The surface morphology of the prepared films were characterized by scanning electron microscopy (SEM, Quanta, FEI) and atomic force microscopy (AFM) Multi-Mode scanning probes Veeco NanoScope IV with a scan area of 2 μm × 2 μm. The chemical composition of the films was investigated by X-ray photoelectron spectrometer (XPS; AXIS ULTRA^{DLD}, Kratos analytical, Manchester, UK). Spectrums were process on software "VISION II" by Kratos analytical, Manchester, UK. The base pressure in the XPS analysis chamber was about 5x10^{-9} torrs. The samples were excited with X-ray hybrid mode 700x300 μm spot area with a monochromatic Al $K_{\alpha\ 1,2}$ radiation at 1.4 keV. X-ray anode was run at 15 kV, 10 mA and 150 W. The photoelectrons were detected with a hemispherical analyzer positioned at an angle of 45^{o} with respect to the normal to the sample surface. Crystallinity composition was characterized by using an X-ray diffractometer (XRD) (Phillips E'pert MPD, Cu-Kα). The crystallite size was determined from XRD peaks using the Scherer equation (Liuxue *et al*., 2006),

$$D=0.9\lambda/\beta\cos\theta_{\beta} \quad (1)$$

where D is crystallite size, λ is the wavelength of X-ray radiation (Cu-Kα = 0.15406 nm), θ is the Bragg's angle and β is the full width at half-maximum (FWHM). The band gap energies of TiO_2 and TiO_2 composites, in powder form, were measured by UV-Vis-NIR Spectrometer with an integrating sphere attachment (Shimadzu ISR-3100 spectrophotometer), by using $BaSO_4$ as reference.

2.3 Photocatalytic reaction test

The photocatalytic activities of TiO_2, SnO_2/TiO_2 and N-doped SnO_2/TiO_2 thin films coated glass fibers were tested by the degradation of 2,4-DCP solution. The 50 mL 2,4-DCP solution with an initial concentration of 10 ppm was treated with 2 g of TiO_2 film coated glass fibers under a UV-lamp (black light) of 110 W powers and 310-400 nm emitted wavelength (Sikong *et al*., 2015). The distance between substrate and light source was 32 cm. The dark reaction chamber had only UV irradiation and reaction times up to 12 h were observed. 2,4-DCP concentration was determined by sampling at certain time intervals and monitoring the absorbance at 284 nm using UV-vis spectrophotometer (UV-1700, Shimadzu, Japan) (Liu *et al*., 2010). The photocatalytic activity of 5 samples was tested and an averaged value was taken for evaluation.

3. Results and Discussion

3.1 XRD result of TiO_2 thin films

The XRD patterns of TiO_2, along with undoped and N-doped SnO_2/TiO_2 thin films, after calcination at 600°C for 2 h, are shown in Fig. 1. Comparisons with the JCPDS 21-1272 anatase card of ASTM (American Society for Testing and Materials), and the JCPDS 21-1276 rutile ASTM card, suggest that all samples had anatase phase. The peaks corresponding to different crystallographic planes against an almost flat base line suggest the formation of polycrystalline compounds (Thomas *et al*., 2002). The very broad

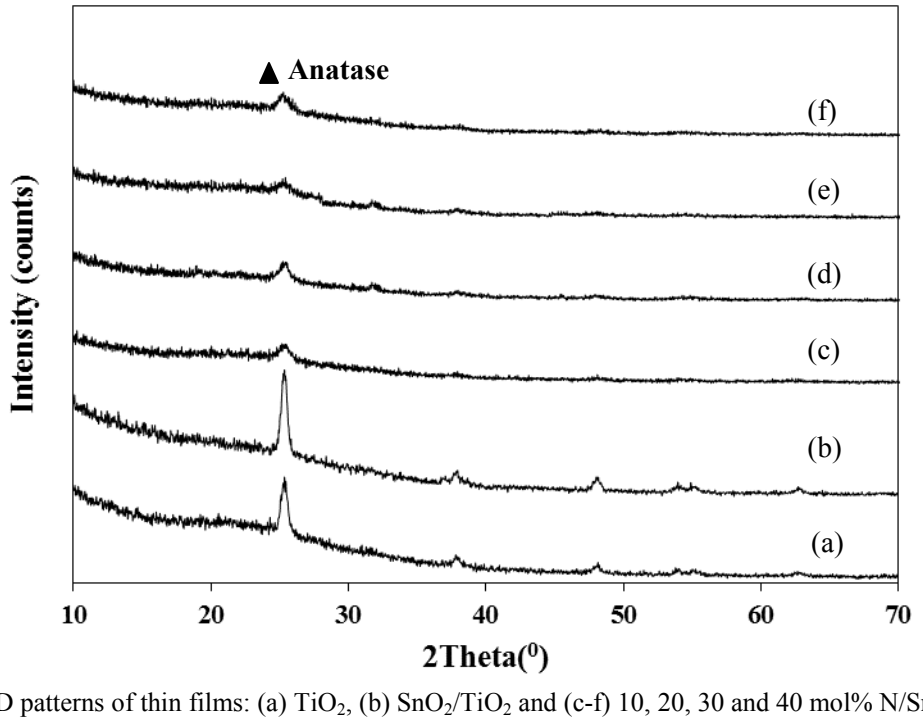

Figure 1. XRD patterns of thin films: (a) TiO_2, (b) SnO_2/TiO_2 and (c-f) 10, 20, 30 and 40 mol% $N/SnO_2/TiO_2$, respectively.

Table 1. Crystallite sizes and energy band gaps of the calcined thin films synthesized

Samples	Crystallite size (nm)	Energy band gap (eV)
TiO_2	17.2	3.20
SnO_2/TiO_2	17.2	3.20
$10N/SnO_2/TiO_2$	12.9	3.06
$20N/SnO_2/TiO_2$	10.3	3.05
$30N/SnO_2/TiO_2$	8.4	3.01
$40N/SnO_2/TiO_2$	8.6	2.94

diffraction peaks at (1 0 1) plane (2θ = 25.3°) of N-doped SnO_2/TiO_2 thin films were due to small crystallite size of TiO_2. The crystallite sizes calculated from Scherrer's equation are shown in Table 1. It is well known that particle sizes play a vital role in photocatalytic activity since smaller crystals offer greater surface area to volume ratios and thus induce better surface absorbability of hydroxyl/water, which in-turn acts as an active oxidizer in the photocatalytic reaction (Yang *et al*., 2010). The relatively broad peaks of the XRD patterns imply the small crystallite size of anatase (Wang *et al*., 2011). The $30N/SnO_2/TiO_2$ composite film calcined at 600°C had the smallest 8.4 nm crystallite size apparently decreased by the N doping. The crystallite size decreased with the N content increased. Nitrogen seems to hinder phase transformation from amorphous to anatase, as $30N/SnO_2/TiO_2$ film had the lowest degree of crystallinity, while SnO_2/TiO_2 had the highest degree (Fig. 1). It can therefore be concluded that the level of nitrogen-doping has a significant effect on the crystallite size of TiO_2 grown during the doping process. It is known that both crystallite size and degree of crystallinity affect photocatalytic activity, so these physical characteristics corroborate the potential of N-doping for such effects.

3.2 Morphology of thin film surface

The morphology of TiO_2 films coated on glass fibers were observed by SEM as illustrated in Fig. 2. It can be seen that the anatase crystallinity nucleated is homogeneous and has a smooth surface. However, excess TiO_2 seems to be randomly deposited on glass fiber surfaces. Agglomeration of nanoparticles was clearly found for SnO_2/TiO_2 film (Fig. 2(f)) but not for undoped TiO_2 (Fig. 2(d)) and $40N/SnO_2/TiO_2$ films (Fig. 2(h)). N-doping hindered the anatase crystal growth and reduced the crystallite size in agreement with the XRD results shown in Fig. 1. The morphology of the composite TiO_2 thin film coating surface observed by AFM illustrated in Fig. 3. It can be seen that crystals of the anatase phase nucleated from the thin film are homogeneous. The average surface roughness of TiO_2, SnO_2/TiO_2 and $40N/SnO_2/TiO_2$ thin film found from AFM images are about 9, 11, and 2 nm, respectively. The SnO_2/TiO_2 thin film exhibits more roughness surface compared with $40N/SnO_2/TiO_2$ and pure TiO_2 films because of the agglomeration of nanocrystallines. It is noted that the grain sizes of pure TiO_2, SnO_2/TiO_2 and $40N/SnO_2/TiO_2$ films are estimated by AFM images about 40-50, 50-60 and 20-30 nm, respectively. This smallest grain size affected by nitrogen-doping promotes the great photocatalytic activity of the $40N/SnO_2/TiO_2$ film.

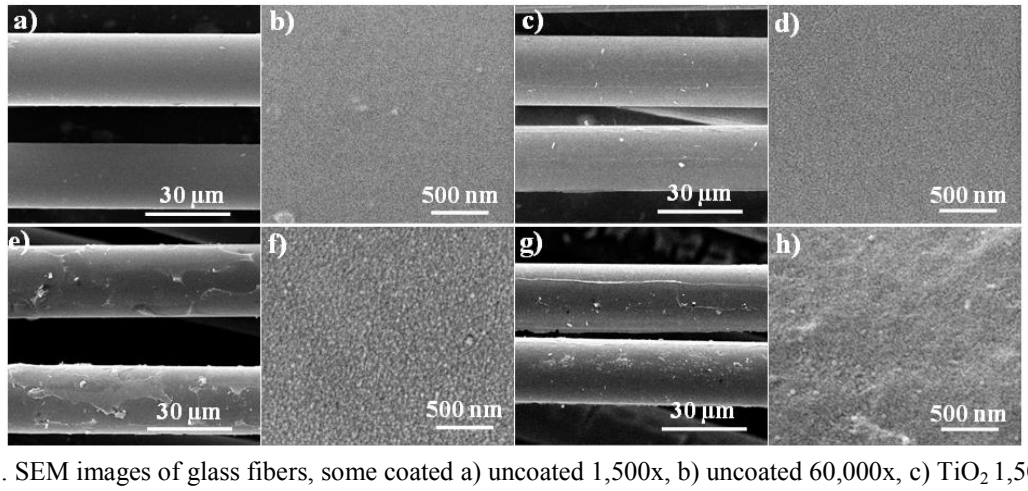

Figure 2. SEM images of glass fibers, some coated a) uncoated 1,500x, b) uncoated 60,000x, c) TiO_2 1,500x, d) TiO_2 60,000x, e) SnO_2/TiO_2 1,500x, f) SnO_2/TiO_2 60,000x, g) $40N/SnO_2/TiO_2$ 1,500x, and h) $40N/SnO_2/TiO_2$ 60,000x.

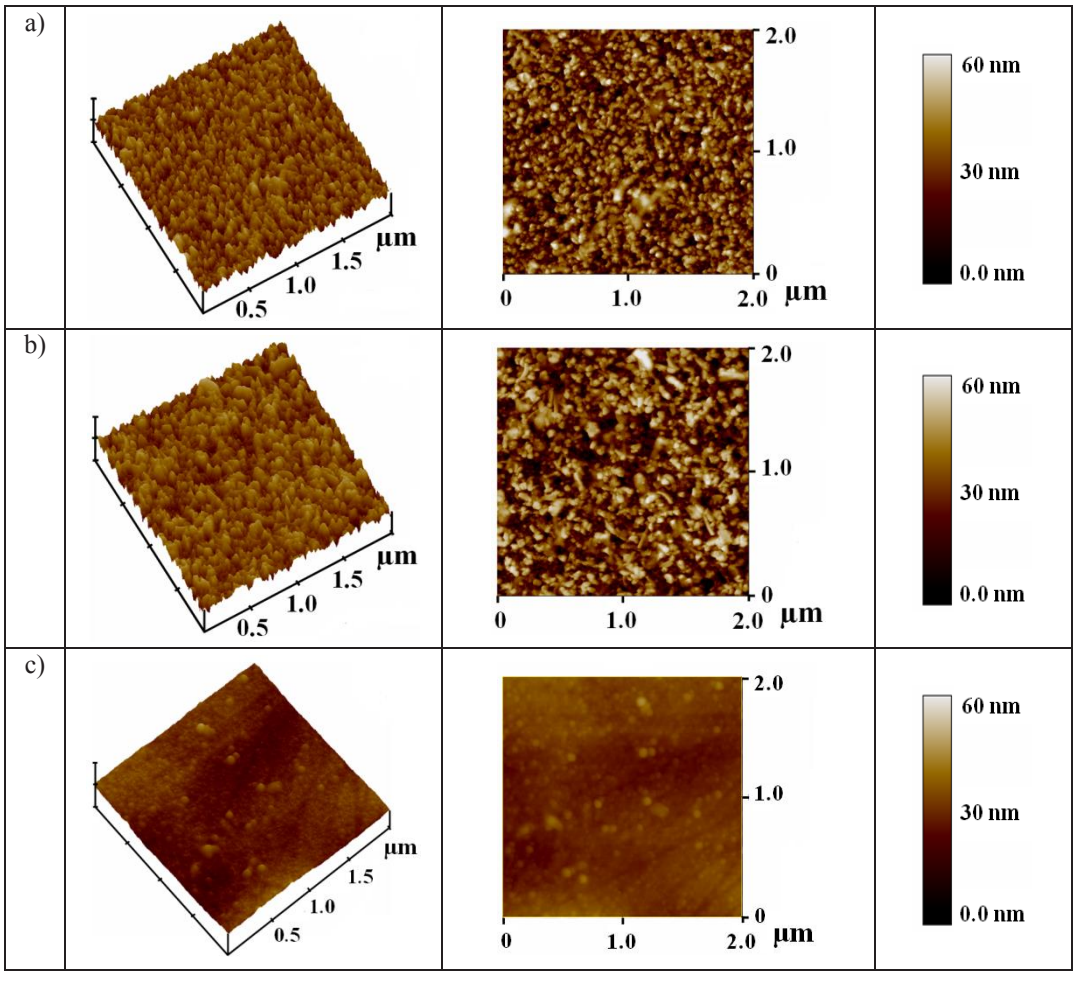

Figure 3. AFM image with a scan area of 2 × 2 µm of a) pure TiO_2, b) SnO_2/TiO_2 and c) $40N/SnO_2/TiO_2$ films coated on glass fibers.

3.3 Band gap energy determination

The UV-vis spectra of pure TiO_2 and composite TiO_2 are shown in Fig. 4. The absorption edge of the samples was determined by the following equation,

$$E_g = 1239.8/\lambda \quad (2)$$

where E_g is the band gap energy (eV) of the sample and λ (nm) is the wavelength of the onset of the spectrum. The undoped TiO_2 catalyst exhibited absorption only in the UV region with the absorption edge around 400 nm. The band gap energies of the N-doped SnO_2/TiO_2 catalysts listed in Table 1 were slightly narrower than that of the undoped TiO_2 (3.20 eV). Dopants affect the UV-vis spectra by inhibiting recombination of electron-hole pairs, here especially for the N-doped specimens. The band gap energy of N-SnO_2/TiO_2 was shifted by 0.14-0.26 eV relative to 3.20 eV for pure TiO_2. The band gap energy of $40N/SnO_2/TiO_2$ was 2.94 eV. The band gap energy of TiO_2 tends to decrease with increasing N content. These shifts demonstrate how photocatalytic activity may be modulated by atomic-level doping of a nano-catalyst. The absorption wavelength of the $40N/SnO_2/TiO_2$ photocatalyst is extended towards visible light (λ = 421.7 nm), relative to the other samples (Sikong *et al*., 2012), giving it the highest photocatalytic activity. The N-doping slightly decreased the band gap to 2.94 eV by the formation of localized N 2p states just above the valence band maximum of TiO_2, due to substitutional N species (Jaiswal *et al*., 2012). When the amount of N-doping increased, the degree of crystallinity of anatase (TiO_2) decreased, resulting in a reduction of crystallite size. In addition, the N interstitial atoms incorporated into the TiO_2 lattice has an effect on the light absorption edge shifting to longer wave length in visible region, leading to the reduction of band gap energy.

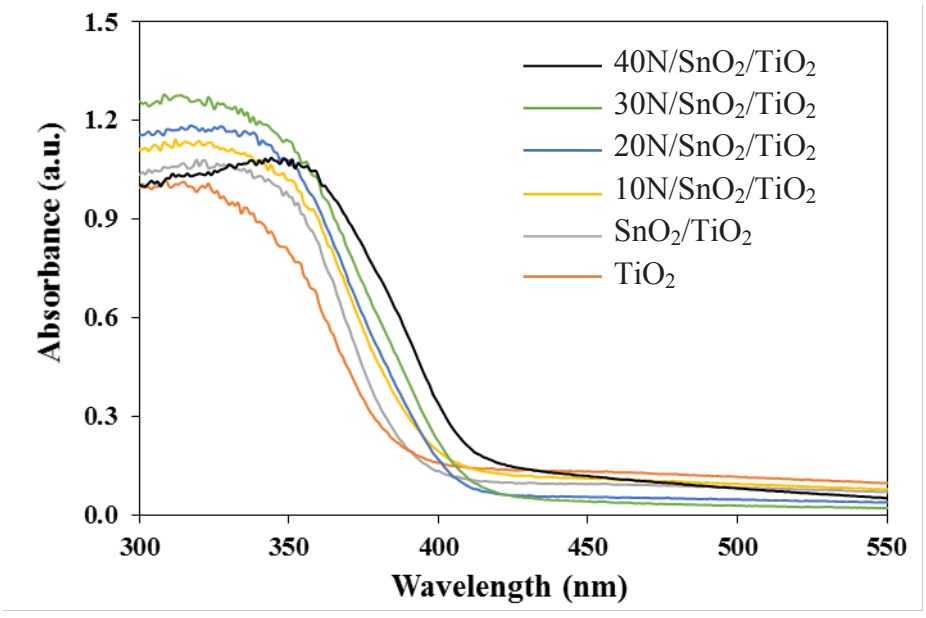

Figure 4. UV-Vis diffuse reflectance spectra of pure TiO_2 and N doped SnO_2/TiO_2 samples.

3.4 XPS analysis

Fig. 5 shows the X-ray photoelectron spectroscopic (XPS) survey spectra of TiO_2 and $40N/SnO_2/TiO_2$ thin films. The elements Ti, O, N, and Sn were clearly detected, and the semi-quantitative analysis estimated atomic fractions in this order were about 16.8, 63.7, 0.5, and 0.7 at%, for the $40N/SnO_2/TiO_2$ thin film. The XPS peaks indicate that the co-doped TiO_2 thin films contain Ti, Sn, O, and N elements, and the binding energies of Ti 2p, Sn 3d, O 1s, and N 1s are 458, 496, 525, and 400 eV, respectively. The Sn 3d XPS peaks of Sn-TiO_{2-x}, shown in Fig. 6(a), demonstrate existence of stannous species on the surface of TiO_2. The Sn $3d_{5/2}$-binding energy of Sn-TiO_{2-x} at 486.1 eV was below the 486.6 eV reference value found inliterature (Xin *et al*., 2009). To assess the state of nitrogen atoms in the $N/SnO_2/TiO_2$ thin films, high-resolution XPS spectra of N 1s region were generated, as shown in Fig. 6(b). The peak at 400.1 eV could be attributed to the interstitial nitrogen atoms in crystal lattice of TiO_2 as Ti-O-N structural feature (Wang *et al*., 2015). This form Ti-O-N linkages, reducing the band gap energy beneficially for the photocatalytic properties of $40N/SnO_2/TiO_2$ films.

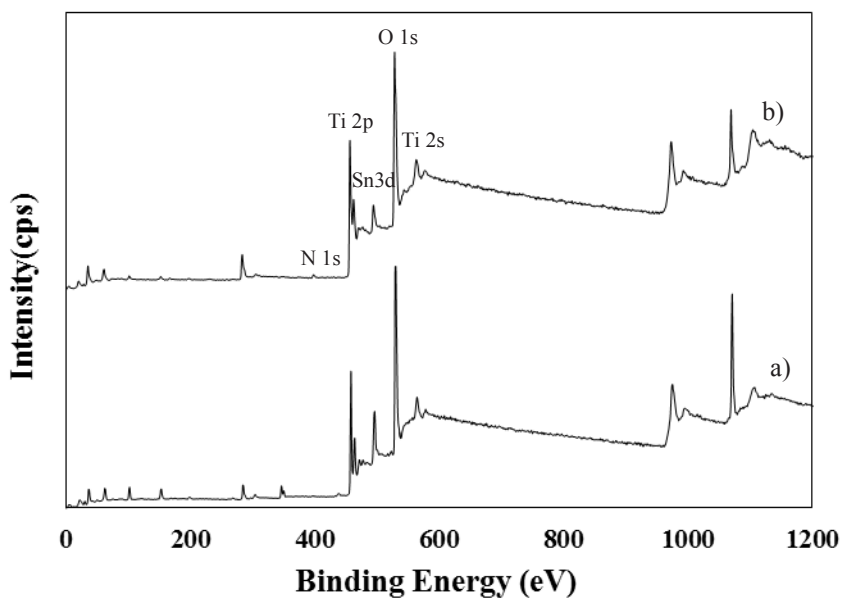

Figure 5. XPS spectra of a) TiO_2 and b) $40N/SnO_2/TiO_2$ thin films samples.

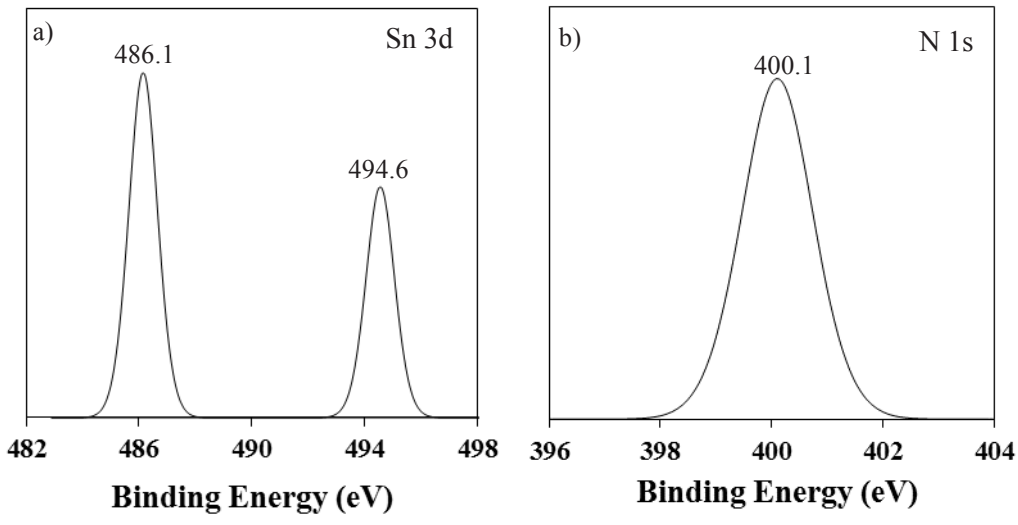

Figure 6. XPS spectrum of a) Sn 3d and b) N 1s on the surface of 40N/SnO_2/TiO_2 thin films samples.

3.5 Photocatalytic activity test

The photocatalytic activities of the films on glass fibers were determined for degradation of 2,4-DCP, with an initial concentration of 10 ppm, under UV light for various irradiation times. The apparent degradation rate constant (k) was chosen as the basic kinetic parameter to compare the photocatalysts. The observed C_0/C vs. irradiation time is plotted in Fig. 7. The fitted k values are shown in Table 2. Where C is the concentration of 2,4-DCP remaining in the solution at irradiation time t, and C_0 is the initial concentration at t = 0. The rate constant k is enhanced by N-doping, and the 0.202 h^{-1} rate constant for the 40N/SnO_2/TiO_2 film is about 4 folds relative to pure TiO_2 under UV irradiation (Fig. 7). The 40N/SnO_2/TiO_2 thin film has optimal photocatalytic activity across the range of compositions tested. According to prior reports, various factors affect the photoactivity of TiO_2 photocatalysts, including crystallinity, grain size, specific surface area, surface morphology and surface state (surface OH radicals), and these factors are not

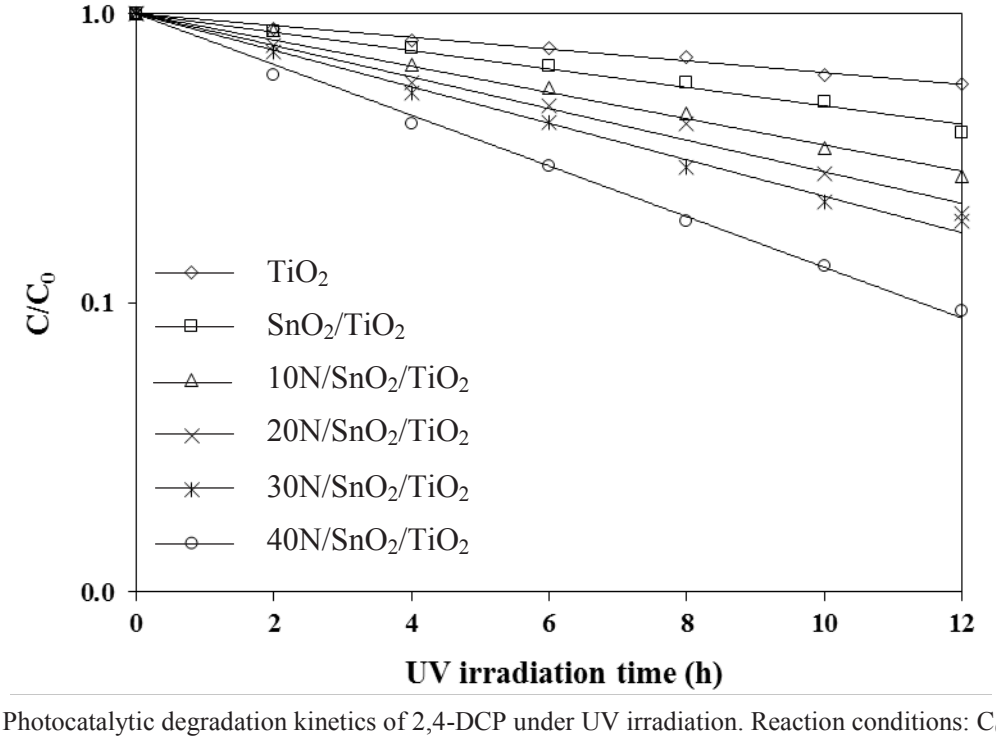

Figure 7. Photocatalytic degradation kinetics of 2,4-DCP under UV irradiation. Reaction conditions: C_0 = 10 ppm, catalyst loading: 2 g, reaction time: 12 h.

Table 2. The identified kinetics of photocatalytic degradation of 2,4-DCP under UV light irradiation

Samples	Rate Equation	Rate constant (k), h^{-1}	R^2
TiO_2	$C = e^{-0.047t}$	0.047±0.002	0.992
SnO_2/TiO_2	$C = e^{-0.073t}$	0.073±0.004	0.988
$10N/SnO_2/TiO_2$	$C = e^{-0.104t}$	0.104±0.002	0.992
$20N/SnO_2/TiO_2$	$C = e^{-0.126t}$	0.126±0.005	0.985
$30N/SnO_2/TiO_2$	$C = e^{-0.145t}$	0.145±0.001	0.993
$40N/SnO_2/TiO_2$	$C = e^{-0.202t}$	0.202±0.001	0.997

independent but closely related to each other (Zaleska *et al*., 2008; Zhang and Liu, 2008). Doping TiO_2 with a suitable amount of nitrogen (40 mol%) in SnO_2/TiO_2 composite films shifted light absorption wavelength to the visible region, reduced crystallite size to be about 8.6 nm, and narrowed the energy band gap to 2.94 eV (Table 1) (Yang *et al.*, 2008). The undoped TiO_2 samples have little ability to degrade the contaminant while the SnO_2/TiO_2 samples modified with nitrogen display higher activity owing to the spectral response in visible light region. Compared to the undoped TiO_2, the N-doped SnO_2/TiO_2 films had a significantly higher degradation, from the spectral response in the visible light region. This is due to the N-doping into the TiO_2 lattice to form an intermediate energy level, and leading to the narrow band gap of N-doped SnO_2/TiO_2 films. Well-crystallized anatase facilitates the transfer of photo-induced vacancies from bulk to surface, for the degradation of organic composites, and effectively inhibits the recombination between photo generated electrons and holes. As seen in Fig. 1, the $30N/SnO_2/TiO_2$ thin film had the smallest crystallite size estimated. It is believed that the photocatalytic degradation reaction of organic pollutants occurs on the surface of TiO_2, and O_2 and H_2O are necessary for the photocatalytic degradation. Under UV irradiation, electron-hole pairs are created on the TiO_2 surface. Oxygen adsorbed on the TiO_2 surface prevents the recombination of electron-hole pairs by trapping electrons of SnO_2 incorporated in TiO_2; Superoxide radical ions ($\cdot O^{-2}$) are thus formed. $\cdot OH$ radicals are formed from holes reacting with either H_2O or OH^- adsorbed on the TiO_2 surface.

4. Conclusions

N-doped SnO_2/TiO_2 composite films were successfully synthesized and deposited on glass fibers, via sol-gel and dip-coating methods. The coated fibers were calcined at 600°C for 2 h at a heating rate of 10°C/min in order to form crystalline anatase. N-doping of SnO_2/TiO_2 composite films affected surface smoothness, crystallite size, and band gap energy of the films. The crystallite size and band gap energy of TiO_2 decreased with the increasing of N content. The synergistic effects of N and SnO_2 co-doping with a suitable amount are responsible for the high photoactivity due to their effect on smaller crystallite size and narrower band gap energy of these TiO_2 composite films. The maximum efficiency of 2,4-DCP degradation was up to 93.65% for 12 h of $40N/SnO_2/TiO_2$ composite film. The $40N/SnO_2/TiO_2$ thin film composite has about 4 times the degradation rate relative to pueTiO_2 under UV irradiation. The results suggest that $40N/SnO_2/TiO_2$ composite thin film is more effective for treating 2,4-DCP contaminated water under UV irradiation.

Acknowledgment

The authors gratefully acknowledge support by the Department of Materials Engineering, Faculty of Engineering and Architecture, Rajamangala University of Technology Isan.

References

Georgieva J, Valova E, Armyanov S, Tatchev D, Sotiropoulos S, Avramova I, Dimitrova N, Hubin A, Steenhaut O. A simple preparation method and characterization of B and N co-doped TiO_2 nanotube arrays with enhanced photoelectrochemical performance. Applied Surface Science 2017; 413(15): 284-91.

Hoseini SN, Pirzaman AK, Aroon MA, Pirbazari AE. Photocatalytic degradation of 2,4-dichlorophenol by Co-doped TiO_2(Co/TiO_2) nanoparticles and Co/TiO_2 containing mixed matrix membranes. Journal of Water Process Engineering 2017; 17: 124-34.

Jaiswal R, Patel N, Kothari DC, Miotello A. Improved visible light photocatalytic activity of TiO_2 co-doped with vanadium and nitrogen. Applied Catalysis B: Environmental 2012; 126: 47-54.

Jian Z, Huang S, Zhang Y. Photocatalytic degradation of 2,4-dichlorophenol using nanosized $Na_2Ti_6O_{13}/TiO_2$ heterostructure particles. International Journal of Photoenergy 2013; 2013: 1-7.

Kadam A, Dhabbe R, Shin DS, Garadkar K, Park J. Sunlight driven high photocatalytic activity of Sn doped N-TiO_2 nanoparticles synthesized by a microwave assisted method. Ceramics International 2017; 43(6): 5164-72.

Kongsong P, Sikong L, Niyomwas S, Rachpech V. Photocatalytic antibacterial performance of glass fibers thin film coated with N-doped SnO_2/TiO_2. The Scientific World Journal 2014; 2014: 1-9.

Li XZ, Zhao BX, Wang P. Degradation of 2,4-dichlorophenol in aqueous solution by a hybrid oxidation process. Journal of Hazardous Materials 2007; 147(1-2): 281-87.

Liu LF, Zhang PH, Yang FL. Adsorptive removal of 2,4-DCP from water by fresh or regenerated chitosan/ ACF/TiO_2. Separation and Purification Technology 2010; 70(3): 354-61.

Liuxue Z, Peng L, Zhixing S. Photocatalysis anatase thin film coated PAN fibers prepared at low temperature. Materials Chemistry and Physics 2006; 98(1): 111-15.

Qin HL, Gu GB, Liu S. Preparation of nitrogen-doped titania with visible-light activity and its application. Comptes Rendus Chimie 2008; 11(1-2): 95-100.

Sikong L, Masae M, Kooptarnond K, Taweepreda W, Saito F. Improvement of hydrophilic property of rubber dipping former surface with $Ni/B/TiO_2$ nano-composite film. Applied Surface Science 2012; 258(10): 4436-43.

Sikong L, Noophum B, Kooptarnond K. Photodegradation of contaminants and antibacterial activity enhanced by AgCl nanoparticles on N, S, Co-doped TiO_2 thin films. Digest Journal of Nanomaterials and Biostructures 2015; 10(2): 455-69.

Sinirtas E, Isleyen M, Soylu GSP. Photocatalytic degradation of 2,4-dichlorophenol with V_2O_5-TiO_2 catalysts: effect of catalyst support and surfactant additives. Chinese Journal of Catalysis 2016; 37(4): 607-15.

Tada H, Konishi Y, Kokubu A, Ito S. Patterned TiO_2/SnO_2 bilayer type photocatalyst. 3. preferential deposition of Pt particles on the SnO_2 underlayer and its effect on photocatalytic activity. Langmuir 2004; 20(9): 3816-19.

Thomas M, Ghosh SK, George KC.Characterisation of nanostructured silver orthophosphate. Materials Letters 2002; 56(4): 386-92.

Valentin CD, Finazzi E, Pacchioni G, Selloni A, Livraghi S, Paganini MC, Giamello E. N-doped TiO_2: Theory and experiment. Chemical Physics 2007; 339(1-3): 44-56.

Wang D, Xiao L, Luo Q, Li X, An J, Duan Y. Highly efficient visible light TiO_2 photocatalyst prepared by sol-gel method at temperatures lower than 300°C. Journal of Hazardous Materials 2011; 192(1): 150-59 .

Wang H, Gao X, Duan G, Yang X, Liu X. Facile preparation of anatase-brookite-rutile mixed-phase N-doped TiO_2 with high visible-light photocatalytic activity. Journal of Environmental Chemical Engineering. 2015; 3(2): 603-08.

Xin B, Ding D, Gao Y, Jin X, Fu H, Wang P. Preparation of nanocrystalline Sn-TiO_{2-X} via a rapid and simple stannous chemical reducing route. Applied Surface Science 2009; 255(11): 5896-901.

Yang J, Bai H, Jiang Q, Lian J. Visible-light photocatalysis in nitrogen-carbon-doped TiO_2 films obtained by heating TiO_2 gel-film in an ionized N_2 gas. Thin Solid Films 2008; 516(8): 1736-42.

Yang G, Jiang Z, Shi H, Xiao T, Yan Z. Preparation of highly visible-light active N-doped TiO_2 photocatalyst. Journal of Materials Chemistry 2010; 20(25): 5301-09.

Zaleska A, Sobczak JW, Grabowska E, Hupka J. Preparation and photocatalytic activity of boron-modified TiO_2 under UV and visible light. Applied Catalysis B: Environmental 2008; 78(1-2): 92-100.

Zhang X, Liu Q. Preparation and characterization of titania photocatalyst co-doped with boron, nickel, and cerium. Materials Letters 2008; 62(17-18): 2589-92.

Zhao BX, Li XZ, Wang P. Degradation of 2,4-dichlorophenol with a novel TiO_2/Ti-Fe-graphite felt photoelectrocatalytic oxidation process. Journal of Environmental Science 2007; 19(8): 1020-24.

Zhou M, Yu J, Liu S, Zhai P, Jiang L. Effects of calcination temperatures on photocatalytic activity of SnO_2/TiO_2 composite films prepared by an EPD method. Journal of Hazardous Materials 2008; 154(1-3): 1141-48.

Received 14 April 2017
Accepted 31 May 2017

Correspondence to
Dr. Peerawas Kongsong
Department of Materials Engineering,
Faculty of Engineering and Architecture,
Rajamangala University of Technology Isan,
744, Sura Narai Rd, Nai Mueng Sub-district,
Mueng Nakhon Ratchasima District,
Nakhon Ratchasima, 30000
Thailand
Email: Physics_PSU@windowslive.com